Heat conduction in 2d nonlinear lattices

Andrea Lippi

and

Roberto Livi[†]

Dipartimento di Fisica dell'Università
L.go E.Fermi 2 I-50125 Firenze, Italy
and Istituto Nazionale di Fisica della Materia, Unità di Firenze
lippi@fi.infn.it, livi@fi.infn.it

Abstract

The divergence of the heat conductivity in the thermodynamic limit is investigated in 2d-lattice models of anharmonic solids with nearest-neighbour interaction from single-well potentials. Two different numerical approaches based on nonequilibrium and equilibrium simulations provide consistent indications in favour of a logarithmic divergence in "ergodic", i.e. highly chaotic, dynamical regimes. Analytical estimates obtained in the framework of linear-response theory confirm this finding, while tracing back the physical origin of this *anomalous* transport to the slow diffusion of the energy of long-wavelength effective Fourier modes. Finally, numerical evidence of *superanomalous* transport is given in the weakly chaotic regime, typically found below some energy density threshold.

Keywords: Heat conduction, Green-Kubo formula, Strong Stochasticity Threshold

PACS numbers: 44.10.+i, 05.45.Jn, 05.60-k, 05.70.Ln

[†] Istituto Nazionale di Fisica Nucleare, Sezione di Firenze

I. INTRODUCTION

The study of heat conduction in models of insulating solids is a long-standing and debated problem. In 1929 R. Peierls provided the first convincing theoretical explanation of this phenomenon, relying upon the hypothesis that lattice vibrations responsible for heat transport in insulating solids can be described as a diluted gas of quantum quasi-particles, the *phonons* [1]. Peierls' model extends Boltzmann's kinetic theory of the classical ideal gas to the phonon gas, by substituting collisions in real space with Umklapp processes in momentum space. Due to the quantum character of this approach, Umklapp processes were theoretically justified as a perturbative effect, epitomizing the scattering of phonons originated by intrinsic features of real solids: disorder and nonlinearity. The main achievement of Peierls' theory is the prediction of the proportionality relation between the thermal conductivity κ and the specific heat at constant volume c_V:

$$\kappa(T) = \frac{1}{3}c_V(T)v\lambda \tag{1}$$

where v and λ are the average velocity and the mean free path of phonons, respectively. Using Debye's formula, the dependence of κ on the temperature T was found to agree with experimental observations in the low-temperature regime. Nonetheless, at least in the high temperature regime, there is no reason why a purely classical model of an insulating solid should not reproduce the correct behaviour of $\kappa(T)$ and Fourier's law

$$\vec{J}(\vec{x}) = \kappa\vec{\nabla}T(\vec{x}) \tag{2}$$

where $\vec{J}(\vec{x})$ and $T(\vec{x})$ are the heat flux and the temperature field, respectively. To our knowledge, the first attempt of its theoretical justification on the basis of a microscopic model of a solid was made in a seminal paper by Rieder, Lebowitz and Lieb [2]. They considered a chain of N coupled harmonic oscillators in contact at its extrema with stochastic thermal baths at different temperatures. They prove that in this simple model of a purely harmonic solid thermal conductivity diverges in the thermodynamoc limit as $\kappa(N) \sim N$. Consistently, the temperature profile in the bulk of the chain is flat. The physical interpretation of these results is that harmonic lattice waves, i.e. Fourier's modes, freely propagate through the lattice, thus contributing to a ballistic rather than diffusive transmission of heat. The same result was obtained numerically for another integrable model, the 1d Toda lattice [3]. Its normal modes, the so-called *Toda solitons*, are nonlinear waves localized in space and also freely propagating through the lattice. More generally, any integrable Hamiltonian system is expected to be characterized by anomalous transport properties since its normal modes, in the perspective of kinetic theory, are equivalent to a "gas" of non-interacting free particles. Following Peierls, the addition of generic disorder and nonlinearity should overtake these anomalies by introducing effective diffusive behaviour. Numerical [4] and analytical [5] estimates performed for the mass-disordered harmonic chain still yield anomalous transport, $\kappa(N) \sim N^{1/2}$, although the temperature gradient was found to be nonzero [6]. Accordingly, disorder is not sufficient to guarantee normal transport properties. It remains nonlinearity, that since the 70's has been widely studied also as a source of chaotic behaviour. In fact, despite its deterministic nature, chaos was shown to yield good statistical properties, namely ergodic behaviour, for most of the thermodinamically relevant observables. Accordingly,

many attempts were made with models of chains of nonlinearly coupled oscillators, that did not achieve convincing conclusions (e.g., see [7–9]). Finally, Casati et al. [10] proposed the ding-a-ling model that exhibits normal heat conductivity. It is worth mentioning that the same result has been confirmed one decade later by Prosen and Robnik [11] for the ding-dong model - a variant of the ding-a-ling one. The great merit of the former paper has been to point out the possibility of obtaining normal conductivity in a nonlinear dynamical model; the latter, thanks also to the increase of computational facilities, has provided convincing evidence of this result by very careful and time consuming numerical simulations. Anyway, in both cases strong chaos has been argued to be the basic mechanism responsible for normal transport properties. In this perspective, one could conjecture that the doubtful results obtained for chaotic potentials, yielding interactions smoother than elastic collisions could deserve extremely lengthy numerical simulations before showing standard transport properties (e.g., see [12,13]).

Unfortunately, the explanation of the above mentioned results is quite different. Both ding-models can be thought as interacting particles bounded to a local, or *substrate*, potential. By substituting the elastic collisions - responsible for the strong chaotic behaviour of these models - with any nonlinear nearest-neighbour interaction potential, numerical evidence of finite thermal conductivity is achieved (for instance, see ref. [14]). Conversely, if the substrate term is absent small wavenumber, i.e. *hydrodynamic*, modes, as a consequence of the conservation of momentum , exhibit a peculiar slow relaxation [15]. This effect can be traced back to the vanishing of the generalized frequency $\omega(k)$ in the limit of small wavenumber, $k \to 0$, characterizing the dispersion relation in presence of an acoustic band [16]. In practice, the frequency associated with the local potential lifts the acoustic band from zero, thus making possible the diffusion of the *hydrodynamic* modes energy. This notwithstanding, it is certainly non-trivial that a purely deterministic chaotic dynamics can give rise to an effective diffusive behaviour. Nonetheless, chaos alone is a necessary but not sufficient ingredient for obtaining normal trasport properties *.

Some progress in the understanding of transport properties in nonlinear lattices has been made recently by exploiting the analogy with the mode-coupling theory, that applies to models of dense fluids rather than diluted gases. Numerical simulations carried out for a 1d lattice with quartic nonlinearity - the Fermi-Pasta-Ulam (FPU) β-model - have shown a power law dependence of the thermal conductivity on the system size: $\kappa \sim N^\alpha$, with $\alpha = 0.39 \pm 0.02$ [16]. This result was obtained for a chain in contact with thermal baths and by equilibrium measurements of κ based on the Green-Kubo formula of linear response theory (for technical details , see also Sec.4). Taking advantage of the results reported in [15], it was possible to conclude that, even for strongly chaotic dynamics, the amplitudes of low wavenumber modes evolve like weakly damped stochastic harmonic oscillators, whose frequencies are *renormalized* w.r.t. the standard harmonic component of the FPU β-model by leading nonlinear terms [18]. On the other hand, large wavenumber modes behave like *fast variables*, governed by a *thermal* behaviour. This is the typical scheme that applies to

---

* We want to point out that normal thermal conductivity has been recently observed also in a class of 1d hamiltonian models without any substrate potential and intercating via nearest-neighbour periodic and double-well chaotic potentials [17].

dense fluids in Fourier space. Self-consistent mode coupling theory (SMT) [19,20] allows one to determine the dependence of κ on N from the integral of the time-correlation function of the total heat flux, yielding in the 1d case the power law

$$\kappa \sim N^{2/5} \tag{3}$$

in very good agreement with numerics. This power-law has been recovered also in many other models of nonlinearly coupled oscillators like the diatomic Toda chain [21,22], the Lennard-Jones (LJ) 6/12 model and the Morse potential [23]. All of these models share one common feature: they are single-well confining potentials. Also in the light of the results recently obtained in [17], the scaling law (3), typical of this class of models, seems to be directly related to this property. It is also worth stressing that, due to its generality, SMT can be extended to determine the dependence of transport coefficients on the system size in higher space dimensions. For the class of models of interest in this paper, it predicts that κ should diverge logarithmically with N in 2d (see Section 4), while in 3d κ is normal, i.e. independent of N.

The aim of this paper is the numerical and analytical study of the thermodynamic limit properties of thermal conductivity κ in the 2d case, by taking into account two examples of single-well confining potentials: the FPU β and the LJ-(6/12) models.

More precisely, in Section 2 we introduce the models and we also discuss some general features of the simplified lattice representation of anharmonic 2d solids used in this paper. In Section 3 we present the results concerning the dependence of κ on N obtained by two different numerical approaches, based on two different definitions of κ. An explicit derivation of the analytical prediction of SMT is worked out in Section 4, where we also discuss the presence of a *superanomalous* divergence of transport coefficients in the weakly chaotic regime, that typically characterizes the above mentioned models for sufficiently small energy [24] (see also [25,26]). Conclusions and perspectives are contained in Section 5.

II. MODELLING HEAT CONDUCTION IN 2D LATTICES

Most of the studies on the heat conduction problem in anharmonic lattices has been devoted to 1d systems. Time-consuming numerical simulations were the main limitation for large scale analysis of this problem in 2d. In fact, only a few contributions have been worked out. For instance in [27] the dependence of the thermal conductivity κ on the temperature T is studied in a 2d triangular lattice of unit mass atoms interacting via a LJ 6/12 potential. Numerical data are consistent with the expected classical law $\kappa \sim T^{-1}$, while the dependence of κ on the system size is not investigated. An interesting contribution in this direction is the paper by Jackson and Mistriotis [12]. The authors compare measurements of κ in 1d and 2d Fermi-Pasta-Ulam (FPU) lattices and they conclude that in both cases there is no evidence that the transport coefficient is finite in the thermodynamic limit. More recent and extended numerical simulations performed for the 2d Toda-lattice [28] have been interpreted in favour of the finiteness of κ in this case.

As usual, numerical analysis alone without any piece of a theory can hardly yield conclusive results. On the other hand, as already stressed in [12], the dependence of κ on the

system size cannot be adequately described by Peierls' model: at least in the high temperature (i.e., classical) limit. the perturbative Umklapp processes cannot account for the genuine nonlinear effects that characterize such a dependence.

The theoretical approach proposed in [16] and careful numerical analysis of 1d systems [18,29], provide a first coherent explanation of the divergence of $\kappa(N)$ in the thermodynamic limit.

In this paper we want to extend this study to 2d systems. For this purpose, let us first describe the adopted lattice model of a homogeneous 2d solid. We consider a square lattice made of $N_x \times N_y$ equal mass (m) atoms. The equilibrium positions of the atoms coincide with the lattice sites, labelled by a pair of integer indices (i, j). Without loss of generality, the lattice spacing a can be set equal to unit and the origin of the cartesian reference frame can be fixed in such a way that $1 < i < N_x$ and $1 < j < N_y$. Accordingly, the 2d-vector of equilibrium position, $\vec{r}_{ij}^{\,0}$, coincides with (i, j). The *short-range* character of interatomic forces in real solids is simplified by assuming that the atoms interact by a nearest-neighbour confining potential $V(\rho)$, that depends on the relative displacement ρ with respect to the equilibrium distance. The natural ordering of the atoms induced by this kind of local interaction allows to identify with the same couple of indices (i, j) the corresponding atom in any dynamical configuration. Specifically, the model is described by the general Hamiltonian

$$H = \sum_{i=1}^{N_x} \sum_{j=1}^{N_y} \left[\left(\frac{|\vec{p}_{ij}|^2}{2m} \right) + V(|\vec{q}_{i+1j} - \vec{q}_{ij}|) + V(|\vec{q}_{ij+1} - \vec{q}_{ij}|) \right] \tag{4}$$

where $\vec{q}_{ij}(t) = \vec{r}_{ij}(t) - \vec{r}_{ij}^{\,0}$, $\vec{r}_{ij}(t)$ is the instantaneous position vector of the (i, j)-atom and $\vec{p}_{ij}(t)$ is the corresponding momentum vector. The time dependence of the canonical variables has been omitted in eq.(4). Without prejudice of generality we set also $m = 1$.

Since we are interested in studying the thermal conductivity κ in this 2d model, we have also to define the relevant physical observables, namely the temperature T_{ij} and the heat flux $\vec{J}_{ij}$. Let us start from the local energy density

$$h(\vec{r}, t) = \sum_{i,j} h_{ij} \delta(\vec{r} - \vec{r}_{ij}) \tag{5}$$

where

$$h_{ij} = \frac{1}{2} |\vec{p}_{ij}|^2 + \frac{1}{4} [V(|\vec{q}_{i+1j} - \vec{q}_{ij}|) + V(|\vec{q}_{ij} - \vec{q}_{i-1j}|) \\ + V(|\vec{q}_{ij+1} - \vec{q}_{ij}|) + V(|\vec{q}_{ij} - \vec{q}_{ij-1}|)] \tag{6}$$

Assuming that local equilibrium holds we obtain immediately a definition of the local temperature T_{ij} by applying the virial theorem:

$$T_{ij} = \langle p_{ij}^{(k)} \frac{\partial h_{ij}}{\partial p_{ij}^{(k)}} \rangle = \langle q_{ij}^{(k)} \frac{\partial h_{ij}}{\partial q_{ij}^{(k)}} \rangle \tag{7}$$

where $k = x, y$ indicates either the x- or the y-component of the corresponding vector variables. The formal definition of the time average symbol is $\langle \bullet \rangle = \lim_{\tau \to \infty} \frac{1}{\tau} \int_0^\tau \bullet \ dt$.

In numerical experiments the time-average must be performed over a finite time span , in general much larger that the local equilibration time.

For hamiltonian (4) one can use the simple expression

$$T_{ij} = \langle p_{ij}^{(x)^2} \rangle = \langle p_{ij}^{(y)^2} \rangle = \frac{\langle p_{ij}^{(x)^2} + p_{i,j}^{(y)^2} \rangle}{2} \tag{8}$$

The heat flux vector is implicitely defined by the continuity equation

$$\dot{h}_{i,j}(t) + \vec{\nabla} \cdot \vec{J}_{ij}(t) = 0 \tag{9}$$

By rewriting this equation in Fourier-space and retaining the leading hydrodynamic contribution (i.e., by applying the large wavelenght limit) one obtains an explicit expression for the components of $\vec{J}$

$$J_{ij}^{(x)} = -\tfrac{1}{4}a \left[f_{ij}^{xx} \left(p_{ij}^{(x)} + p_{i+1j}^{(x)} \right) + f_{ij}^{yx} \left(p_{ij}^{(y)} + p_{i+1j}^{(y)} \right) \right]$$
$$J_{ij}^{(y)} = -\tfrac{1}{4}a \left[f_{ij}^{xy} \left(p_{ij}^{(x)} + p_{ij+1}^{(x)} \right) + f_{ij}^{yy} \left(p_{ij}^{(y)} + p_{ij+1}^{(y)} \right) \right] \tag{10}$$

where the components of the local vector forces are defined as follows

$$f_{ij}^{xx} = -\frac{\partial V\left[|\vec{q}_{i+1j} - \vec{q}_{ij}|\right]}{\partial q_{ij}^{(x)}} \qquad f_{ij}^{yx} = -\frac{\partial V\left[|\vec{q}_{i+1j} - \vec{q}_{ij}|\right]}{\partial q_{ij}^{(y)}}$$

$$f_{ij}^{xy} = -\frac{\partial V\left[|\vec{q}_{ij+1} - \vec{q}_{ij}|\right]}{\partial q_{ij}^{(x)}} \qquad f_{ij}^{yy} = -\frac{\partial V\left[|\vec{q}_{ij+1} - \vec{q}_{ij}|\right]}{\partial q_{ij}^{(y)}}$$

It is worth defining also the space-time average of the heat flux vector

$$\langle \vec{J} \rangle = \langle \frac{\sum_{i,j} \vec{J}_{ij}}{N_x N_y} \rangle \tag{11}$$

that will be widely used in the following Sections.

Finally, since we are interested to investigate thermodynamic limit properties, we should impose periodic boundary conditions (pbc), that are the standard choice for reducing as much as possible undesired boundary effects on bulk properties.

III. MODELS AND NUMERICAL EXPERIMENTS

The numerical simulations that we are going to describe in this Section have been performed for two different single-well potentials:

$$V_1(\rho) = \frac{1}{2}\rho^2 + \frac{\beta}{4}\rho^4 \qquad , \qquad Fermi - Pasta - Ulam \quad \beta - model \tag{12}$$

$$V_2(\rho) = \frac{A}{\rho^{12}} - \frac{B}{\rho^6} + \frac{B^2}{4A} \qquad , \qquad Lennard - Jones \quad 6/12 \quad model \tag{13}$$

The reasons for this twofold choice are the following:

6

- analyzing heat tansport in the 2d version of the widely studied case of potential V_1;

- verifying the theoretical prediction (see next Section) that nearest-neighbour single-well nonlinear potentials exhibit the same kind of dependence of $\kappa(N)$ in the large N limit;

- investigating the possible consequences on transport properties of the slowing-down of relaxation below the so called *Strong Stochasticity Threshold*, that was measured for potential V_2 in [24].

It is worth stressing that V_1 does not contain any natural energy and length scales; all numerical simulations with this potential have been performed with $\beta = 10^{-1}$ and with an integration time step $\Delta t = 10^{-2}$, that is two orders of magnitude smaller than the minimum harmonic period $(\tau_{min} = \pi/\sqrt{2})$.

At variance with V_1, V_2 is characterized by natural length and energy scales, the equilibrium distance $r_0 = (2A/B)^{1/6}$ and the well depth $W = B^2/4A$, respectively. In order to make the two models as close as possible we have chosen the parameters A and B in such a way that the coefficients of the second and fourth order terms of the Taylor series expansion of V_2 around its minimum coincide with those of V_1, thus obtaining $r_0 \approx 25$, $W \approx 8.6$ and $\tau_{min} = \pi r_0^4/(6\sqrt{2}B) \approx 2.2$. In numerical experiments we have adopted a time step $\Delta t = 5 \cdot 10^{-3}$, that guarantees a sufficient sampling of the integration algorithm especially when strong nonlinearities are explored by the dynamics.

Numerical measurements of the thermal conductivity κ as a function of the lattice size N have been performed under nonequilibrium and equilibrium conditions: the former are inspired by an ideal experiment for the verification of Fourier's law (2), the latter stem from linear response theory (see Sec. 4). Both approaches are theoretically equivalent; nonetheless, their comparison on a numerical ground is quite instructive.

Nonetheless, this kind of numerical simulations are quite heavy, so that any trick for saving CPU time is worth to be applied. Since we are interested in investigating thermo-dynamic limit properties we have to perform measurements keeping the ratio $R = N_y/N_x$ constant. On the other hand, there is *a priori* no reason for choosing $R = 1$. In fact, we have checked that reliable measurements of κ can be obtained in lattices with $R < 1$. As an example, in Fig.1 we show the dependence of κ on N_y for $N_x = 128$ and for potential V_2, in the presence of thermal baths acting on the boundary atoms at temperatures $T_L = 1$. and $T_R = 0.5$ (details are given in the next subsection). After a sharp increase for small values of N_y thermal conductivity κ reaches a plateau already for $N_y \approx 20$.

This preliminary analysis has been performed for both potentials V_1 and V_2 in nonequilibrium and in equilibrium simulations: we have concluded that $R = 1/2$ is a reasonable compromise, valid in all of these cases.

A. Nonequilibrium measurements of thermal conductivity

A straightforward way of measuring thermal conductivity κ amounts to simulate numerically a true experiment where the atoms at the left and right edges of the 2d lattice are coupled with two thermal baths at different temperatures T_L and T_R. This setting restricts the application of *pbc* to the direction orthogonal to the temperature gradient: we impose

pbc along the y-axis, while the boundary atoms are coupled to a rigid wall through the force link with the missing atom in the x-direction.

Various models of thermal baths, either stochastic or deterministic ones, are at disposal. The results of numerical simulations reported in this paper have been obtained by using the Nosé-Hoover deterministic model [30,31] [†]. It has two advantages with respect to stochastic algorithms: it can be easily implemented as an ordinary differential equation and it reduces the residual thermal impedence effects at the lattice boundaries.

The equations of motion are

$$
\begin{aligned}
\dot{\vec{q}}_{ij} &= \vec{p}_{ij} \\
\dot{\vec{p}}_{ij} &= -\frac{\partial V}{\partial \vec{q}_{ij}} - (\delta_{i,1} + \delta_{i,N_x})\zeta_{ij}\vec{p}_{ij} \\
\dot{\zeta}_{1j} &= \frac{1}{\theta^2}\left[\frac{|\vec{p}_{1j}|^2}{2T_L} - 1\right] \\
\dot{\zeta}_{N_xj} &= \frac{1}{\theta^2}\left[\frac{|\vec{p}_{N_xj}|^2}{2T_R} - 1\right]
\end{aligned}
\tag{14}
$$

where δ is the Kronecker symbol. In practice, the integration scheme (14) has been implemented by a standard fourth order Runge-Kutta algorithm. Note that each boundary atom is coupled through the momentum equation to its thermal bath variable ζ, that guarantees local thermal equilibrium at temparature T_L and T_R on the left and right boundaries, respectively.

Starting from random initial conditions after a sufficiently long transient time stationary nonequilibrium evolution is eventually approached. According to the heat equation (2), a constant thermal gradient should establish through the lattice in the x-direction and $\langle J^{(x)} \rangle > 0$, while $\langle J^{(y)} \rangle = 0$. Here, the symbol $\langle \bullet \rangle$ indicates the time average over stationary nonequilibrium states. The time span, over which good convergence of the time-average is obtained, increases with N_x: for instance, $\mathcal{O}(10^5)$ integration steps are sufficient for $N_x = 16$, while for $N_x = 128$ this time grows up to $\mathcal{O}(10^7)$.

The occurrence of stationary nonequilibrium conditions can be checked by verifying the equality

$$
|\langle \vec{J} \rangle| = \langle J_M \rangle = -\langle \frac{1}{N_y}\sum_{j=1}^{N_y}\zeta_{Mj}|\vec{p}_{Mj}|^2\rangle \qquad , \qquad M = 1, N_x
\tag{15}
$$

where the r.h.s. is the average heat flux flowing through the boundaries. Despite in numerical simulations finite time-averages never yield exactly $\langle J^{(y)} \rangle = 0$, one finds that $|\langle \vec{J} \rangle|$ is very well approximated by $\langle \vec{J}^{(x)} \rangle$.

Some of the stationary temperature profiles obtained for different values of N_x for potential V_1 and V_2 are shown in Figures 2 and 3, respectively. The values of the temperature T_i have been averaged also in space over all the N_y atoms with abscissa $x = i$:

[†] We have checked that other models of thermal baths, in particular stochastic ones, yield the same kind of results reported in this paper.

$$T_i = \frac{1}{N_y} \sum_{j=1}^{N_y} T_{ij} \tag{16}$$

It is worth stressing that the local temperature T_{ij} is a time-averaged quantity (see eq.(8)) over the stationary nonequilibrium evolution.

The lattice length has been rescaled to unit in order to verify the overlap of the profiles for increasing values of N_x: in both cases we observe a good data collapse for $N_x > 32$ indicating that the temperature gradient in the thermodynamic limit vanishes as

$$\vec{\nabla} T_i \sim N_x^{-1} \tag{17}$$

In the FPU β-model the temperatures of the thermal baths, $T_L = 20$ and $T_R = 10$, have been chosen for obtaining good ergodic properties of the dynamics, i.e. fast relaxation to local equilibrium. Boundary effects of thermal impedence induced by the coupling with the thermal baths are reduced for increasing values of N_x. The temperature gradient looks quite close to a constant, but a more careful inspection shows that the profile has a slight curvature. The effect is even more evident for the Lennard-Jones model, whose temperature profiles converge to an s-shaped curve. In particular, thermal impedence at the boundaries seems to persist also in the large N_x limit, despite the smaller values of $T_L = 1$ and $T_R = 0.5$, that already guarantee ergodicity for this model. Such deviations from Fourier's law indicate that nonlinearities influence boundary effects and also the dependence of κ on the temperature. On the other hand, we are interested in extracting the scaling of κ with the system size N_x. It can be obtained on the basis of Fourier's law and eq.(17) by plotting the quantity $\langle J^{(x)} \rangle N_x \sim \kappa$ versus N_x (see Figures 4 and 5). For both 2d models we find evidence of a logarithmic scaling of κ with N_x.

B. Equilibrium measurements of thermal conductivity

The above described nonequilibrium measurements of the heat transport coefficient κ have been made keeping T_L and T_R constant for increasing values of N_x. The data collapse of the temperature profiles implies also that in the thermodinamic limit, $N_x \to \infty$, the temperature gradient in the bulk of the chain drops to zero. Accordingly, for increasing values of N_x nonequilibrium measurements are expected to reproduce better and better linear response conditions. The Green-Kubo linear response theory [32] provides an alternative definition of κ with respect to the one contained in Fourier's law. More precisely, a general expression of the heat conductivity tensor for a solid contained in a volume V is given by the formula

$$\kappa_{\mu\nu} = \frac{V}{K_B T^2} \int_0^\infty \langle J^{(\mu)}(t) J^{(\nu)}(0) \rangle dt \tag{18}$$

where K_B is the Boltzmann constant and the time correlation function of the heat flux components along the μ and ν directions is averaged over equilibrium states at temperature T. Note that the symbol $\langle \bullet \rangle$ indicates now the equilibrium ensemble average.

In our models of homogeneous 2d nonlinear solids the thermal conductivity corresponds indifferently to anyone of the diagonal components of the transport coefficient tensor defined in (18). In particular we have chosen to measure

$$\kappa \equiv \kappa_{xx} = \frac{RN_x^2}{K_B T^2} \lim_{t \to \infty} \int_0^t \langle J^{(x)}(\tau) J^{(x)}(0) \rangle d\tau \qquad (19)$$

where $J^{(x)}$ is the x-component of the space-averaged heat flux vector (11). As in nonequilibrium measurements fixing the ratio $R = N_y/N_x = 1/2$ is a good compromise for reducing CPU time, while maintaining reliable asymptotic estimates of κ.

We have performed numerical simulations at constant energy density, e, by eliminating the thermal bath variables ζ's from eq.(14). Periodic boundary conditions have been imposed also in the x-direction, so that the 2d lattice becomes a torus. In practice the integration scheme has been implemented by a fourth order Maclachlan-Atela symplectic algorithm [33], that is more appropriate than a Runge-Kutta one for this kind of *microcanonical* simulations.

The expression on the r.h.s of eq.(19) can be evaluated numerically for finite values of t. Accordingly, we define a "finite time" thermal conductivity $\kappa(t)$ by removing from eq.(18) the limit operation $t \to \infty$. In order to reduce fluctuations, the heat flux time-correlation function has been averaged over a sufficiently large set of random initial conditions, extracted from the microcanonical probability distribution. For sufficiently large values of t both models (12) and (13) exhibit a logarithmic divergence of $\kappa(t)$. As an example, in Figure 6 we report the case of the Lennard-Jones (6-12)-model. Despite highly time consuming simulations have been performed for averaging over initial conditions, in this example fluctuations are still persistent for large values of t. This notwithstanding, numerical data are compatible with the expected logarithmic divergence.

According to the argument reported in [16] this divergence in time can be assimilated to a divergence with the system size N_x. In fact, numerical estimates of the time-correlation function of the local heat flux, $C_i(\tau) = \langle J_{0j}(\tau) J_{ij}(0) \rangle$ show that in single-well nonlinear potentials, due to the "rigidity" of low-wavenumber modes (see next Section), the energy propagates with the velocity of sound in a nonlinear medium (see also [15]):

$$\tilde{c} = \sqrt{(1 + \alpha(E))} c \qquad (20)$$

where c is the velocity of sound due to the harmonic component of the nonlinear potential and the renormalization factor $\alpha(E) > 0$ introduces a dependence of $\tilde{c}$ on the total energy, indicating its nonlinear character. We have verified that these features are common to the potentials (12) and (13).

The evaluation of $\kappa(t)$ for finite time t in the Green-Kubo integral can be assimilated to an estimate of the divergence with the system size by the formal relation $t = N_x/\tilde{c}$. In this sense, equilibrium simulations confirm the results of nonequilibrium ones.

IV. TRANSPORT IN STRONG AND WEAK CHAOTIC DYNAMICS

The conjecture that deterministic chaos is an efficient mechanism for ergodic behaviour has been extensively investigated by numerical experiments in many degrees of freedom Hamiltonian systems, like those introduced in Section 2. One of the main issues is that, for sufficiently high energy density e, the time averages of most observables of thermodynamic interest rapidly approach the expectation value predicted by equilibrium ensembles. This notwithstanding, below a specific value e_T - the so-called Strong Stochasticity Threshold

(*SST*) (see [25,26] and the references therein contained) - the equilibration time may increase dramatically, despite the persistence of deterministic chaos. It is not our aim, here, to discuss why such a slow relaxation mechanism typically occurs in these models. We just want to stress that their *mild* nonlinear character make them quite different from *mathematically* standard chaotic models like K- or A-systems. In fact, the results obtained in [15] show that regularities are present even above the SST. More precisely, in a 1d FPU chain the amplitudes of low-k Fourier modes are found to evolve like weakly damped and forced harmonic oscillators. Dissipation and forcing epitomize the complex nonlinear mechanism of energy exchange among the modes and they are found to vanish in the limit $k \to 0$. One can argue that these can be only an effect induced by global, i.e. *hydrodynamic*, conservation laws of total momentum and energy. In this sense, such a behaviour is expected to be present in any space dimension d, although the possibilities of energy exchanges among the modes are expected to become more and more efficient for increasing values of d. These remarks suggests that, in a nonlinear model of a solid, Fourier modes can be assimilated to a dense fluid rather than to a diluted gas, as in Peierls' phonon theory.

A. Analytical estimate of anomalous thermal conductivity above the SST

Relying upon the above conjecture, strongly supported by numerical simulations, we want to derive an analytical estimate of the thermodynamic limit behaviour of thermal conductivity κ for 2d single-well anharmonic lattices. In practice, here we explicitly extend to the 2d case the method introduced in [16] and described in detail for the 1d case in [34].

The amplitudes of the Fourier modes in a 2d square lattice have the standard expression

$$\vec{Q}_{\vec{k}} = \frac{1}{\sqrt{N_x N_y}} \sum_{m=1}^{N_x} \sum_{n=1}^{N_y} \vec{q}_{mn} e^{-i\left(\frac{2\pi}{N_x}k_x m + \frac{2\pi}{N_y}k_y n\right)} \tag{21}$$

where $\vec{q}_{mn}$ is the canonical space coordinate and the 2d wave-vector $\vec{k}$ has components $k_x = -\frac{N_x}{2}\ldots\frac{N_x}{2}$ and $k_y = -\frac{N_y}{2}\ldots\frac{N_y}{2}$. We consider an isolated hamiltonian model of the type (4); the equations of motion expressed in terms of Fourier amplitudes and their canonically conjugated momenta $\vec{P}_{\vec{k}}$ read

$$\dot{\vec{Q}}_{\vec{k}} = \vec{P}_{\vec{k}}$$
$$\dot{\vec{P}}_{\vec{k}} = -\omega_{\vec{k}}^2 \vec{Q}_{\vec{k}} + \sum_{\vec{k} \neq \vec{k}'} \vec{F}_{\vec{k}\vec{k}'} \tag{22}$$

where $\omega_{\vec{k}}$ obeys the dispersion relation [‡]

$$\omega_{\vec{k}}^2 = 4\left[\sin^2 \frac{\pi k_x}{N_x} + \sin^2 \frac{\pi k_y}{N_y}\right] \tag{23}$$

[‡]For he sake of simplicity we have set $\omega_0 = \left(\frac{\partial^2 V}{\partial r^2}\right)_{r=r_0} = 1$

$F_{\vec{k}\vec{k}'}$ is the formal expression of the nonlinear interaction force between modes $\vec{k}$ and $\vec{k}'$.

Numerical experiments show that low-k Fourier modes behave like *slow* dynamical variable, whose relaxation time scales are much longer than those of high-k modes, that play the role of *fast* variables. This analogy with hydrodynamic properties of dense fluids suggests the application of SMT [19,20].

Since the hydrodynamic behaviour is ruled by low-k modes, the first step amounts to project the dynamics onto the subspace of slow variables $(\vec{Q}^s_{\vec{k}}, \vec{P}^s_{\vec{k}})$ by a proper projection operator

$$\mathcal{P}^s X = \sum_{\vec{k}} \left[\frac{\langle X \cdot \vec{Q}^{s*}_{\vec{k}} \rangle}{\langle |\vec{Q}^s_{\vec{k}}|^2 \rangle} \vec{Q}^s_{\vec{k}} + \frac{\langle X \vec{P}^{s*}_{\vec{k}} \rangle}{\langle |\vec{P}^s_{\vec{k}}|^2 \rangle} \vec{P}^s_{\vec{k}} \right] \tag{24}$$

According to linear response theory the equations of motion can be casted in the form [34]:

$$\dot{\vec{Q}}^s_{\vec{k}} = \vec{P}^s_{\vec{k}}$$
$$\dot{\vec{P}}^s_{\vec{k}} = -\tilde{\omega}^2_{\vec{k}} \vec{Q}^s_{\vec{k}} - \int_0^t \Gamma_{\vec{k}}(t-t') \vec{P}^s_{\vec{k}}(t') dt' + \vec{R}_{\vec{k}} \tag{25}$$

where $\vec{R}_{\vec{k}} = (1 - \mathcal{P}^s)\dot{\vec{P}}^s_{\vec{k}}$ is the effective force, that is related by the dissipation-fluctuation theorem to the memory kernel as follows:

$$\Gamma_{\vec{k}}(t) \propto \langle \vec{R}_{\vec{k}}(t) \cdot \vec{R}_{\vec{k}}(0) \rangle \tag{26}$$

Note that in the projected equations of motion the harmonic frequency $\omega_{\vec{k}}$ is renormalized to the energy dependent frequency

$$\tilde{\omega}_{\vec{k}} = \sqrt{(1 + \alpha(E))}\omega_{\vec{k}} \tag{27}$$

where

$$\alpha(E) = \frac{1}{\beta} \frac{\int \delta(H - E) d\vec{r}}{\int r^2 \delta(H - E) d\vec{r}} - 1 \tag{28}$$

In the last formula we have introduced the microcanonical average by assuming that equilibrium properties are practically guaranteed by the fast thermalization of high-k modes. As observed also in [15] the projected slow variables can be interpreted as "nonlinear" Fourier modes, whose frequency is renormalized by anharmonic contributions. Numerical simulations support this approach also thanks to the remarkable quantitative agreement with the theoretical prediction (27).

The projected equations of motion have a clear theoretical interpretation but they are practically useless for working out analytical calculations. We have to introduce some simplifying hypotheses. We suppose that the time scale of slow hydrodynamic variables can be unambiguously separated form the typical microscopic time scales: specifically, this amounts to reduce the memory kernel Γ to a δ distribution and the fluctuating force $\vec{R}$ to a stochastic force. By introducing an explicit complex-variable representation of the mode amplitudes,

$$\vec{Q}_{\vec{k}} = \vec{A}_{\vec{k}} + i\vec{B}_{\vec{k}}$$

we rewrite the set of equations (25) in the approximate form of standard stochastic equations:

$$\ddot{\vec{A}}_{\vec{k}} + \gamma_{\vec{k}}\dot{\vec{A}}_{\vec{k}} + \tilde{\omega}_{\vec{k}}^2 \vec{A}_{\vec{k}} = \vec{\xi}_{\vec{k}}$$
$$\ddot{\vec{B}}_{\vec{k}} + \gamma_{\vec{k}}\dot{\vec{B}}_{\vec{k}} + \tilde{\omega}_{\vec{k}}^2 \vec{B}_{\vec{k}} = \vec{\eta}_{\vec{k}} \tag{29}$$

where $\gamma_{\vec{k}}$ can be interpreted as an effective dissipation coefficient, while fluctuations are now assumed to be represented by gaussian white noise processes:

$$\langle \vec{\xi}_{\vec{k}}(t)\vec{\xi}_{\vec{k}'}(t') \rangle \propto \delta_{\vec{k}\vec{k}'}\delta(t - t')$$
$$\langle \vec{\eta}_{\vec{k}}(t)\vec{\eta}_{\vec{k}'}(t') \rangle \propto \delta_{\vec{k}\vec{k}'}\delta(t - t') \tag{30}$$

It is convenient to introduce the scalar variable

$$W_{\vec{k}} = \dot{\vec{A}}_{\vec{k}} \cdot \vec{B}_{\vec{k}} - \vec{A}_{\vec{k}} \cdot \dot{\vec{B}}_{\vec{k}} \tag{31}$$

that satisfies the Langevin type equation:

$$\dot{W}_{\vec{k}} = -\gamma_{\vec{k}} W_{\vec{k}} + \zeta_{\vec{k}} \tag{32}$$

where

$$\langle \zeta_{\vec{k}}(t)\zeta_{\vec{k}'}(t') \rangle \propto (|\vec{A}_{\vec{k}}|^2 + |\vec{B}_{\vec{k}}|^2)\delta_{\vec{k}\vec{k}'}\delta(t - t')$$

According to the definition (11) the average heat flux vector can be thought as the sum of a harmonic term and an anharmonic one, $\vec{J}_H$ and $\vec{J}_A$, respectively. The harmonic term is obtained by considering only the forces given by the quadratic part of the interaction potential: simple calculations show that its components can be written in the form:

$$J_H^{(x)} = \sum_{k_x,k_y} c_{k_x}\omega_{k_x} W_{\vec{k}}$$
$$J_H^{(y)} = \sum_{k_x,k_y} c_{k_y}\omega_{k_y} W_{\vec{k}} \tag{33}$$

where

$$\omega_{k_{x,y}} = 2\left|\sin\frac{\pi k_{x,y}}{N_{x,y}}\right| \qquad , \qquad c_{k_{x,y}} = \frac{N_{x,y}}{\pi}\frac{d\omega_{k_{x,y}}}{dk_{x,y}}$$

In close analogy with the renormalization of the effective frequency of slow variables, it can be shown that the leading contribution to $\vec{J}_A$, stemming from the anharmonic part of the interaction potential, is proportional to $\vec{J}_H$ through an energy (and also model) dependent factor $C(E)$, i.e. $\vec{J}_A = C(E)\vec{J}_H$. For instance, the expression of $C(E)$ in the FPU β-model (12) is

$$\frac{1}{N_x N_y}\sum_{\vec{k}} \omega_{\vec{k}}^2 \left(\left|\vec{A}_{\vec{k}}\right|^2 + \left|\vec{B}_{\vec{k}}\right|^2\right) \tag{34}$$

Summarizing, the components of the average heat flux vector can be expressed in general by the proportionality relations

$$J^{(x)} \propto \sum_{k_x,k_y} c_{k_x}\omega_{k_x} W_{\vec{k}}$$
$$J^{(y)} \propto \sum_{k_x,k_y} c_{k_y}\omega_{k_y} W_{\vec{k}} \tag{35}$$

Assuming the validity of the generalized equipartiton theorem

$$\omega_{\vec{k}}^2 \langle |A_{\vec{k}}|^2 \rangle = \omega_{\vec{k}}^2 \langle |B_{\vec{k}}|^2 \rangle = \mathcal{U}(E) \tag{36}$$

where $\mathcal{U}(E)$ is a function of the energy E, and using the solution of (32), one can obtain an analytical estimate of the heat flux time-correlation function present in the Green-Kubo integral (18):

$$\langle J_H^i(t) J_H^i(0) \rangle \sim \mathcal{U}(E) \sum_{\vec{k}} c_{k_i}^2 e^{-\gamma_{\vec{k}} t} \sim \int_0^{2\pi} d\theta \int_0^{\pi} \frac{dk}{(2\pi)^2} k c^2(k\cos\theta) e^{-\gamma(k)t} \tag{37}$$

where the last expression is obatined by assuming that in the thermodynamic limit the summation can be approximated by an integral.

The explicit dependence of the dissipation coefficient γ on the modulus of the wave-vector $\vec{k}$ is provided by SMT [19,20]. Specifically, it predicts that the time-correlation functions of hydrodynamic modes decay in time as follows:

$$G(k,t) \simeq e^{-\omega(k)t} \tag{38}$$

where the $\omega(k)$ are complex generalized frequencies ruling the oscillatory and relaxation behaviour of the hydrodynamic modes. For 2d homogeneous systems they depend just on $k = |\vec{k}|$ and their explicit expression in the hydrodynamic limit, $k \to 0$, is found to be

$$\omega(k) \simeq i\tilde{c}k + \nu k^2 \ln k \tag{39}$$

where $\tilde{c}$ is the velocity of sound in the homogeneous medium and the second addendum of the r.h.s. is the dissipation term $\gamma(k) = \mathcal{R}e(\omega(k))$. Substituting into eq.(37) and retaining only the leading contribution to the function $c(k\cos\theta)$ in the limit $k \to 0$, one obtains the estimate

$$\langle J_H^i(t) J_H^i(0) \rangle \propto \int_0^{\pi} \frac{dk}{2\pi} k e^{-tk^2 \ln k} \sim \frac{1}{t} + \mathcal{O}\left(\frac{1}{t \ln t}\right) \tag{40}$$

Accordingly, the heat conductivity κ is predicted to diverge as $\ln t$ in the $t \to \infty$ limit in 2d lattices.

It is worth stressing that SMT predicts also that $\gamma(k) \sim k^{5/3}$ in 1d systems, yielding a diverging heat conductivity $\kappa \sim N^{2/5}$ in the thermodynamic limit. The very good agreement with numerical experiments (see [16]) strengthen the conjecture that the anomalous properties of transport coefficients in nonlinear lattice models stems from the hydrodynamic nature of low-k effective modes. Said differently, total energy and momentum conservation laws impose on models with single-well potentials a dispersion relation yielding a subdiffusive behaviour of the energy exchange among these modes and, consequently, ill-defined transport coefficients. On the other hand, SMT predicts that in 3d the Green-Kubo integral is convergent so that κ becomes a well defined quantity.

This dependence on the space dimension and the generality of predictions (at least for what concerns the class of single-well nonlinear potentials) make this piece of theory quite elegant and physically sound.

B. The effect of weak chaos on anomalus transport

All the numerical simulations presented in Section 3 have been performed in the strong chaotic regime of the dynamics. In this case ergodic behaviour occurs quite rapidly on the microscopic time scale, with the exception of hydrodynamic modes, whose slow relaxation, due to macroscopic conservation laws, rules the observed divergence of transport coefficients. In the above theoretical treatment this corresponds to the assumption that time-correlation functions can be estimated on the basis of equilibrium ensemble averages.

On the other hand, we know that below the SST relaxation to equilibrium may slow-down dramatically for most of the physically interesting observables. According to the results reported in [26] the heat flux is expected to belong to this class of observables. Then, we expect also that in such a dynamical regime the transport mechanism can be significantly modified.

We have checked this conjecture by considering model (13), whose SST has been estimated [24] at a value of the energy density

$$e_{SST} = 0.3 \tag{41}$$

in the units adopted in this paper. We have performed numerical simulations with thermal baths at temperature $T_L = 0.1$ and $T_R = 0.05$ for different values of N_x verifying the data collapse of the temperature profiles. Following the same approach described in Section 3.1 we have estimated the dependence of the thermal conductivity on N_x. We find evidence of a power-law divergence

$$\kappa \sim N_x^\alpha \tag{42}$$

with $\alpha = 0.77$ (see Fig.7). Note that below the SST the exponent α is a function of the energy density e.

The power law divergence of κ below the SST is confirmed by the numerical estimate of the Green-Kubo integral. In Fig. 8 we compare dependence of κ on time t for $e = 0.1$ and for $e = 3.0$, below and above the SST, respectively. The comparison of the two curves in a linear versus logarithmic scale shows that the asymptotic behaviour of $\kappa(t)$ is completely different in the two chaotic dynamical regimes. In particular, for $e = 3.0$ we recover a logarithmic divergence, while for $e = 0.1$ we find a power law divergence $\kappa(t) \sim t^\alpha$ with $\alpha = 0.75$.

For what concerns the interpretation of this last result, one has to observe that for a sufficiently long time equilibrium conditions will be eventually approached. The asymptotic time dependence of the Green-Kubo integral should turn to the logarithmic growth on any finite system. The relevance of this *superanomalous* effect could be established only by evaluating the dependence of the relaxation time on the system size. Estimates obtained for relatively small size systems seem to indicate that the crossover time between the power-law and the logarithmic behaviour of the Green-Kubo integral icreases more than linearly with the system size N_x. On the other hand, as we have often pointed out along this paper, numerics may can provide crucial insight for the understanding of these phenomena, but cannot be assumed as a proof of anything. Since this effect might have very interesting physical consequences we hope to work out in the near future an analytical approach apt to describe the *superanomaly* of transport coefficients below the SST.

V. CONCLUSIONS AND PERSPECTIVES

The presence of anomalous thermal conductivity in 2d lattices of atoms coupled by nonlinear nearest-neighbour single-well potentials has been verified by numerical experiments and analytical estimates. According to SMT, the effect of dimensionality is found to make the thermodynamic limit power-law divergence of 1d models turn to a logarithmic divergence of 2d models, thus confirming the soundness of the general theoretical framework worked out to interpret such anomalous properties emerging from strongly chaotic dynamics [16,34]. It is also worth mentioning that in this dynamical regime 3d models are predicted to exhibit normal transport properties, i.e. finite thermal conductivity.

In this paper we have also pointed out that a superanomalous behaviour ruled by a power-law divergence of the thermal conductivity, seems to characterize transport properties of 2d models below the SST. Such a behaviour has been observed also in 1d systems where the crossing of the SST corresponds to an increase of the power from the value 2/5 towards the limit value 1, that is expected to be approached for vanishing energy densities (i.e. in the harmonic limit). Here we have decided to report just the results for 2d systems, where the comparison between the power-law and the logarithmic divergence stresses the effect of the extremely slow relaxation mechanism already observed almost half a century ago in the seminal numerical experiment by E. Fermi, J. Pasta and S. Ulam [35].

At present we are not able to conclude just on the basis of numerical simulations if superanomalous transport is a finite size effect or an asymptotic property, that could even concern 3d systems. Also in this case, the construction of a suitable theoretical approach would greatly help in answering to this interesting question.

REFERENCES

[1] R.E. Peierls, *Quantum theory of solids*, Oxford University Press, London (1955).

[2] Z. Rieder, J.L. Lebowitz and E. Lieb, J. Math. Phys. **8**, 1073 (1967).

[3] F. Mokross and H. Büttner, J. Phys. C **16**, 4539 (1983).

[4] K. Ishii and H. Matsuda, Prog. Theor. Phys. Suppl. **45**, 56 (1970)

[5] J.B. Keller, G.C. Papanicolaou, J. Weilenmann, Comm. Pure and App. Math. **32**, 583 (1978).

[6] A. Casher and J.L. Lebowitz, J. Math. Phys. **12**, 1701 (1971); A.J. O'Connor and J.L. Lebowitz, J. Math. Phys. **15**, 692 (1974).

[7] N. Nakazawa, Progr. Theor. Phys. Suppl. **45**, 231 (1970);

[8] D.N. Payton, M. Rich, W.M. Visscher, Phys. Rev. **160**, 706 (1967);

[9] W.M. Visscher *Methods in Computational Physics* , Academic Press, New York, (1976).

[10] G. Casati, J. Ford, F. Vivaldi, W.M. Visscher, Phys. Rev. Lett. **52**, 1861 (1984).

[11] T.Prosen, M. Robnick, J. Phys. A **25** 3449 (1992).

[12] E. A. Jackson, A. D. Mistriotis, J. Phys. Condens. Matter **1** 1223 (1989).

[13] H. Kaburaki, M. Machida, Phys. Lett. A **181**, 85 (1993);

[14] B. Hu, B.-W. Li and H. Zhao, Phys. Rev. E **57**, 2992 (1998);

[15] C. Alabiso, M.Casartelli, P.Marenzoni, J. Stat. Phys. **79**, 451 (1995).

[16] S. Lepri, R. Livi, A. Politi, Europhys. Lett. **43**, 271 (1998).

[17] C. Giardiná, R. Livi, A. Politi and M. Vassalli, University of Florence, preprint 1999.

[18] S. Lepri, R. Livi, A. Politi, Phys. Rev. Lett. **78**, 1896 (1997).

[19] Y. Pomeau, R. Résibois, Phys. Rep. **19** 63 (1975).

[20] M.H. Ernst, Physica D **47** 198 (1991).

[21] T. Hatano, Phys. Rev. E **59**, R1 (1999).

[22] M. Vassalli, Diploma Thesis, University of Florence 1998.

[23] A. Lippi, Diploma Thesis, University of Florence 1999.

[24] G. Benettin and A. Tenenbaum, Phys. Rev. A **28**, 3020 (1983).

[25] L. Casetti, R. Livi, A. Macchi and M. Pettini, Europhys. Lett. **32**, 549 (1995).

[26] C. Giardinà and R. Livi, J. Stat. Phys. **91**, 1027 (1998).

[27] R.D. Mountain and R.A. MacDonald, Phys. Rev. B **28**, 3022 (1983).

[28] N. Nishiguchi, Y. Kawada and T. Sakuma, J. Phys.: Condens. Matter **4**, 10227 (1992).

[29] S. Lepri, R. Livi and A. Politi, Physica D **119**, 140 (1998).

[30] S. Nosé, J.Chem Phys. **81**, 511 (1984).

[31] W.G. Hoover, Phys. Rev. A **31**, 1695 (1985).

[32] R.Kubo, M.Toda, N. Hashitsume, *Statistical Physics II*, Springer Series in Solid State Sciences, Vol. 31 (Springer, Berlin 1991).

[33] R.I. Maclachlan and P. Atela, Nonlinearity **5**, 541 (1992).

[34] S. Lepri, Phys. Rev. E **58**, 7165 (1998).

[35] E. Fermi, J. Pasta and S. Ulam, Los Alamos report LA-1940 (1955); reprinted in E. Fermi, *Collected Papers*, Vol. II (Univ. of Chicago Press, Chicago, 1965), p. 978 .
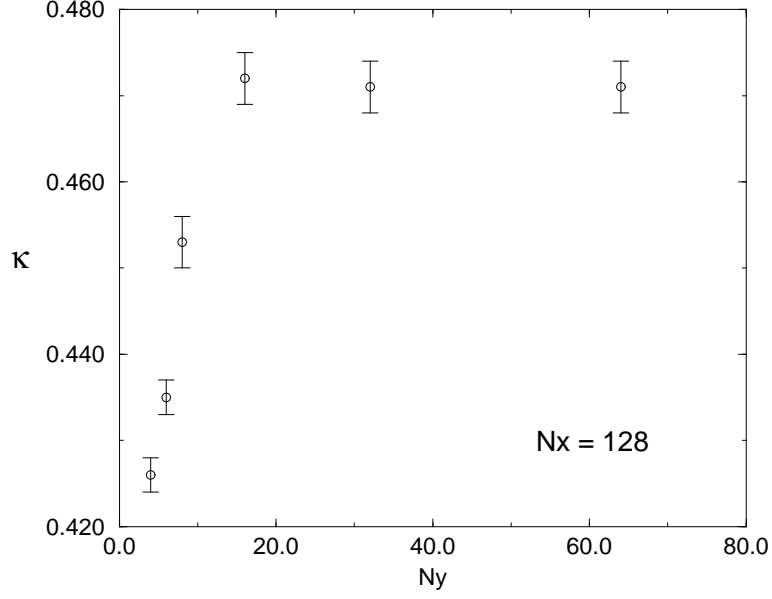
FIG. 1. The thermal conductivity κ versus N_y for the Lennard-Jones potential (13) with $N_x = 128$, $T_L = 1.$ and $T_R = 0.5$.
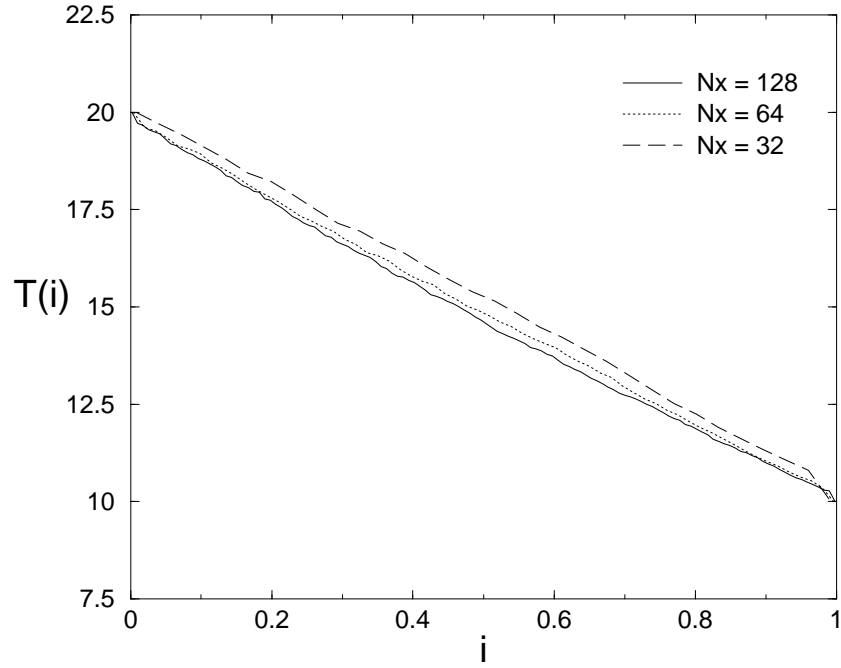

FIG. 2. Temperature profiles of the 2d FPU-β model for different values of N_x
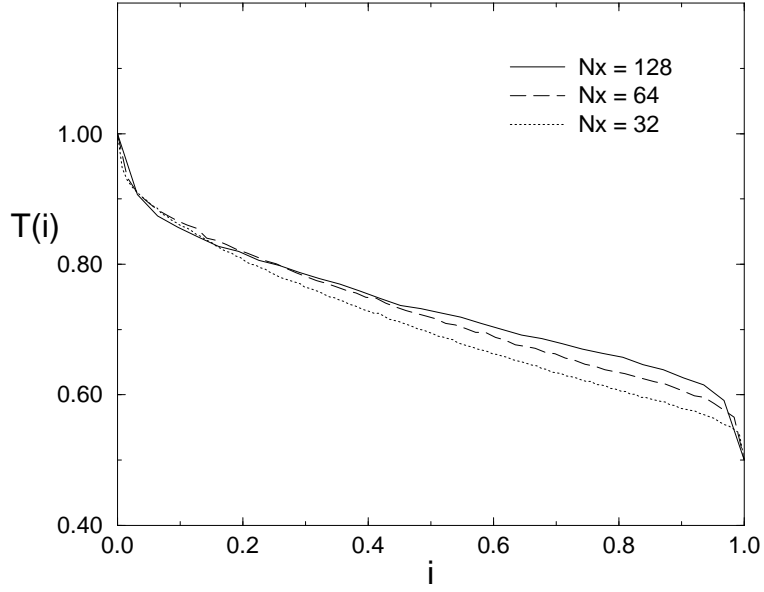
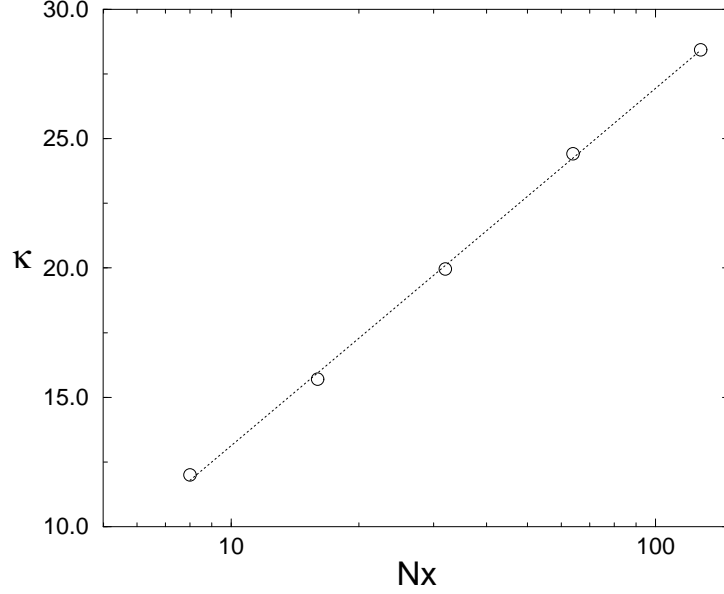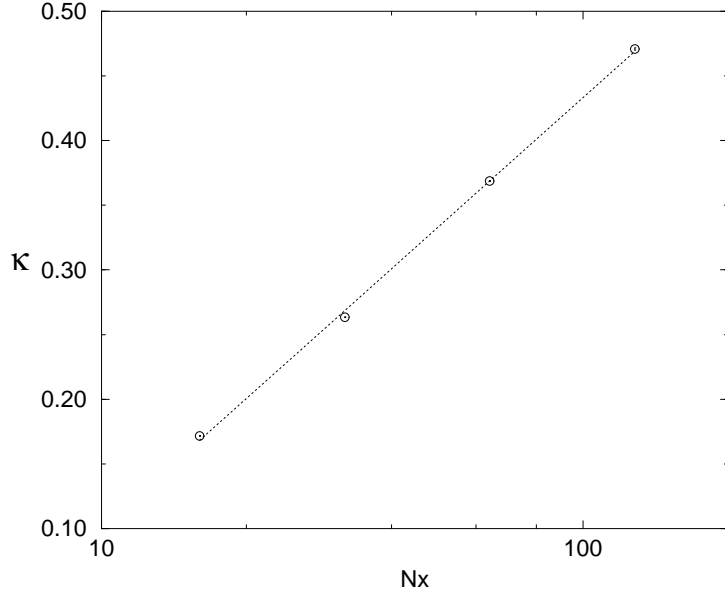FIG. 3. Temperature profiles of the 2d Lennard-Jones 6/12 model model for different values of N_x

FIG. 4. Dependence of the thermal conductivity κ on the system size N_x for the FPU β-model; $T_L = 20.$ and $T_R = 10.$. Statistical errors have the size of the symbols and the dotted line is the best fit.

FIG. 5. Dependence of the thermal conductivity κ on the system size N_x for the Lennard-Jones (6/12)-model; $T_L = 1.$ and $T_R = 0.5$. Statistical errors have the size of the symbols and the dotted line is the best fit.
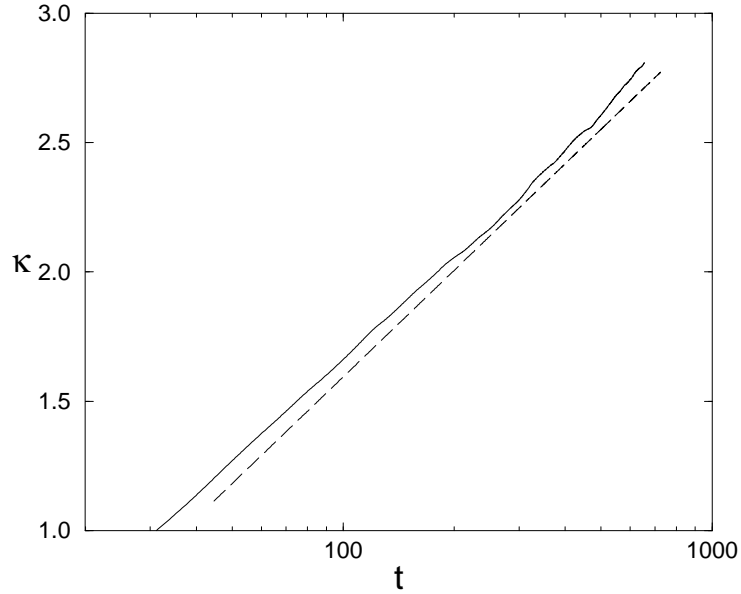

FIG. 6. The finite-time thermal conductivity $\kappa(t)$ versus time t for the LJ (6/12)-model with $N_x = 64$ and $e = 1.5$. The curve has been obtained by averaging over 100 initial conditons. The dashed straight line has been drawn just for comparison with numerical data.
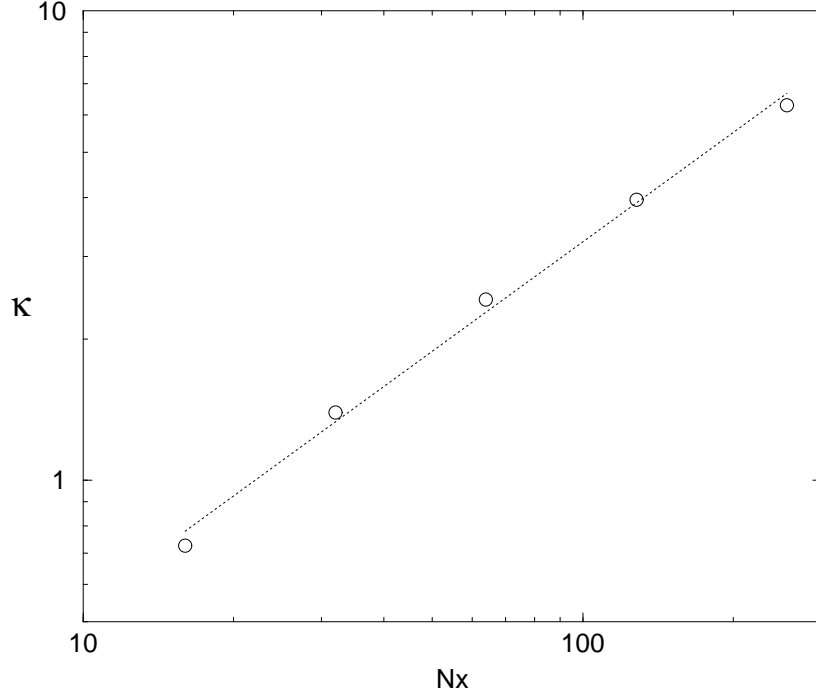
FIG. 7. The thermal conductivity κ versus the system size N_x with $T_L = 0.1$ and $T_R = 0.05$ for the LJ (6/12)-model. The dotted line is a best fit for the power law $\kappa \sim N_x^{\alpha}$ yielding $\alpha \simeq 0.77\pm0.03$.
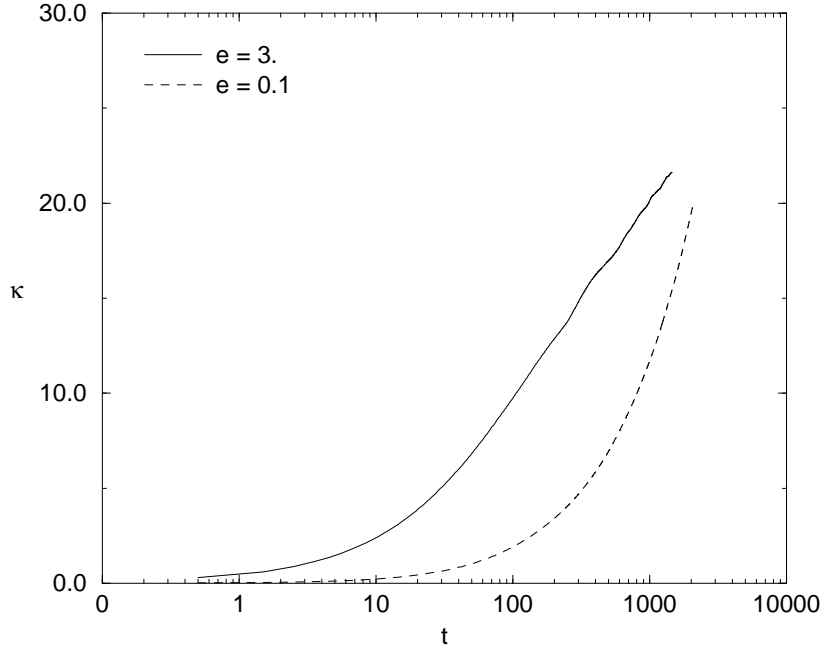

FIG. 8. The finite-time thermal conductivity κ versus time t for the LJ (6/12)-model with $N_x = 64$ below ($e = 0.1$) and above ($e = 3.0$) the SST.